Numerical modeling of internal waves within a coupled analysis framework and their influence on spar platforms

Nishu V. Kurup[*1], Shan Shi[1a], Lei Jiang[1b] and M.H. Kim[2c]

[1]*Offshore Dynamics, Inc. 16225 Park Ten Place Drive, Suite 500, Houston, TX, 77084, USA*
[2]*Department of Ocean/Civil Engineering, Texas A&M University, College Station, TX, 77843, USA*

Abstract. Internal solitary waves occur due to density stratification and are nonlinear in nature. These waves have been observed in many parts of the world including the South China Sea, Andaman Sea and Sulu Sea. Their effect on floating systems has been an emerging field of interest and recent offshore developments in the South China Sea where several offshore oil and gas discoveries are located have confirmed adverse effects including large platform motions and riser system damage. A valid numerical model conforming to the physics of internal waves is implemented in this paper and the effect on a spar platform is studied. The physics of internal waves is modeled by the Korteweg-de Vries (KdV) equation, which has a general solution involving Jacobian elliptical functions. The effects of vertical density stratification are captured by solving the Taylor Goldstein equation. Fully coupled time domain analyses are conducted to estimate the effect of internal waves on a typical truss spar, which is configured to South China Sea development requirements and environmental conditions. The hull, moorings and risers are considered as an integrated system and the platform global motions are analyzed. The study could be useful for future guidance and development of offshore systems in the South China Sea and other areas where the internal wave phenomenon is prominent.

Keywords: internal waves; KdV equation; coupled analysis; spar platforms; mooring tension; offset

1. Introduction

Although essentially an underwater phenomenon, surface manifestations of internal waves have been known to sailors as "deadwater phenomenon" or "tidal rips". Korteweg and de Vries (1895) provided the first rigorous theoretical description of internal waves based on the Boussinesq approximation to Navier-Stokes equations. There has been extensive literature on the physical and theoretical aspects of these waves (Duda and Farmer 1999, Ostrovsky and Stepanyants1989) as well as reports of their effects on deepwater platforms (Osbourne *et al*. 1977).

The study on the effects of these waves on offshore platforms is an emerging area of interest. Previous works include a study on the effects of internal waves on offshore drilling units (Kurup *et*

∗Corresponding author, Senior Engineer, E-mail: nishu.kurup@deepoil.com
[a] Ph.D., E-mail: shan.shi@deepoil.com
[b] E-mail: lei.jang@deepoil.com
[c] Professor, E-mail: m-kim3@tamu.edu

al. 2010) and impact of waves on FLNG offloading operations (Xu *et al*. 2013). Zhang and Li (2007) and Sun and Huang (2012) have also presented work on the effects of internal waves on offshore platforms such as spars and semisubmersibles using a simplified hyperbolic secant model.

Additionally Huang *et al* (2015) has studied the effects of internal waves on spar platforms based on theories proposed by Miyati (1985) and Chio and Cammasa (1999). However the effects of internal waves on a spar platform within a coupled analysis framework where the hull, moorings and risers are considered as an integrated system have not been studied before and thus are presented in this paper. A theoretical model for internal wave due to Apel (2003) and Gurevich and Pitaevskii (1973a, b) is presented and implemented within a coupled analysis hydrodynamic program. The effects of these waves on spar platforms are then studied and conclusions drawn. This kind of platform/mooring/riser coupled interaction with internal waves is hard to be model tested in wave tanks since the internal wave generation is probably one of the most difficult things to do in the relevant experiments. Under such circumstances, the system safety and robustness with internal waves could only be verified through reliable numerical simulation tools as in the present study.

2. Physics of internal waves

Internal waves could be weakly or strongly nonlinear. The characteristic shape and properties of internal waves are governed by nonlinear effects as well as the dispersive effects of the medium. The nonlinearity increases the wave velocity towards a shock like condition while the dispersive nature of the medium causes the dissipation of the pent-up energy thus leading to the formation of a soliton or solitary wave train.

Internal waves have three different phases: generation, propagation and dissipation. The generation phase has not been fully understood due to its complexity. However it is known that the formation of a pycnocline on the side of a continental shelf or sill due to tidal flows could be a source for these waves (Armi and Farmer 1988). The propagation phase is primarily considered in this paper as it is during this phase that the waves interact with the platform. This phase is characterized by the addition of oscillations over time and a decrease in amplitude, phase speed and wavelength along the wave from the front to the trailing edge. The dissipation phase differs for sill based and shelf based waves with the latter suffering from the effects of bottom interactions and thus losing more energy.

3. Analytical model

A complete understanding of internal waves will require a solution to the full Navier-Stokes equations in 3-D but considering the spatial scale of the phenomenon the computational effort will be time consuming. Thus analytical models are usually developed for the analysis of internal waves.

A few approximations are adopted in the formulation of the theoretical model and are thought to be acceptable since the purpose of the current paper is to examine the generic effects of internal waves on spar platforms. We assume that the ocean consists of two layers and the wavelength is long compared to the upper water depth. In addition the two dimensional quadratic Korteweg-de Vries equation for weakly nonlinear waves is implemented in this study. This theory assumes that

the ratio of the amplitude to the upper layer depth is small. While a higher order theory can capture some of the effects neglected by the current assumptions, previous work (Koop and Butler 1981, Segur and Hammack 1982) has shown that the effect on wave velocities are not significant and thus the current formulation should suffice to study the effects on offshore platforms. In addition there are formulations which capture the physics due to finite depth or deep water assumptions (Benjamin 1966, Ono 1975, Joseph 1977, Kubota *et al.* 1978, Liu *et al.* 1985) and while the effects on offshore structures due to these theories will be interesting, this is deferred to later work.

The effect on internal waves on OTEC platforms was studied by Shan *et al.* (2013). The study focused on the influence of the enhanced drag due to the vortex induced vibrations (VIV) of the CWP. It was found that there was significant influence due to internal waves on the VIV enhanced drag coefficient envelope. However since fatigue is not considered in this paper the effect of VIV due to internal wave is not modeled in the current analysis. Design considerations influenced by fatigue might require the consideration of VIV due to internal wave.

The coordinate system used in the following section has the origin at the sea surface with x being the horizontal distance from the source and z the vertical distance. The 2D equations presented can be extended to 3D by a simple rotation of the coordinate system.

The Boussinesq approximation, which assumes that small density variations can be neglected in all terms except the buoyancy term, can be applied for internal waves to simplify the Navier – Stokes equation. It is in fact the buoyancy term that is significant for the formulation of the internal wave. Further simplifications and approximations to the Boussinesq approximation yields the two dimensional quadratic Korteweg-de Vries equation (Korteweg and de Vries 1895).

$$\frac{\partial \eta}{\partial t} + c_0 \frac{\partial \eta}{\partial x} + c_0 \gamma \frac{\partial^3 \eta}{\partial x^3} + \alpha \eta c_0 \frac{\partial \eta}{\partial x} = 0 \tag{1}$$

where η is the amplitude of the internal wave, c_0 is the long wavelength phase speed and γ and α are environmental parameters describing the dispersion and nonlinearity respectively. This equation describes weakly nonlinear waves which is the focus of the current paper. Multiple solutions exist for this equation two of which were presented in the original paper by Korteweg and Vries (1895). These solutions while interesting from the theoretical point of view failed to fully replicate the observed characteristics of internal waves.

The solution presented in this paper was first derived in the context of collisionless plasma waves by Gurevich and Pitaevskii (1973a, b) and was extended to study internal waves in oceans by Apel (2003). The solution in terms of Jacobian elliptic functions is termed the dnoidal model for internal waves. The relevant model is presented here without derivations. The reader is referred to the relevant papers mentioned above for the derivation of the solution by asymptotic methods. The wave profile is of the form

$$\eta(x,t) = 2\eta_0 \left\{ dn_s^2 \left[\frac{1}{2} k_0 (x - Vt) \right] - 1 + s^2 \right\} \tag{2}$$

where *s* is the elliptic modulus of the Jacobian elliptic function and varies from 0 to 1. η_0 is the wave amplitude. The parameters k_0 and *V* are calculated in terms of the *KdV* environment variables as follows

$$k_0 = 2\sqrt{\left(\frac{\alpha \eta_0}{6\gamma} \right)} \tag{3}$$

$$V = c_0 \left(1 + \frac{1+s^2}{3} \alpha \eta_0 \right) \tag{4}$$

The variation of the elliptic parameter s was originally derived in terms of the space time ratio τ where

$$\tau = \frac{x - c_0 t}{\alpha \eta_0 c_0 t} \tag{5}$$

As τ varies from -1 to 2/3, s varies from 0 to 1. Since the original solution in terms of complete elliptic integrals is seen to be analytically noninvertible a simpler formulation in terms of the error function can be utilized.

$$s^2 = \frac{erf[\beta(\tau - \varphi)] + 1}{2} \tag{6}$$

where β and φ are parameters that govern the distribution of wavelengths and number of oscillations over the wave packet under consideration. These values are obtained from observations of internal waves.

The original solution is further amended to account for the effect of the pycnocline and the recovery of the pycnocline to the equilibrium position. The first effect is captured by a vertical structure function $W(z)$ which is the eigenfunction of the well known Taylor Goldstein equation with rigid boundary conditions applied at the top and bottom.

$$\frac{d^2 W(z)}{dz^2} + \left(\frac{N^2}{(U-c)^2} - \frac{U_{zz}}{(U-c)} - k^2 \right) W(z) = 0 \tag{7}$$

where N is the buoyancy frequency, U is the background current velocity, c is the phase speed and k is an wavenumber. This equation has solutions in the form of multiple modes which are numerically evaluated by matrix methods. The recovery of the pycnocline is captured by a recovery function $I(x,t)$ given as

$$I(x,t) = 1 + tanh\left[\frac{2A(x - Vt - \chi)}{x_a} \right] \tag{8}$$

where A, χ and x_a are parameters that control the shape of the recovery function.

The *KdV* environmental parameters can be obtained by coupling the Taylor Goldstein equation with the equations from the Boussinesq approximation. In this paper the special case of a two layered fluid is considered where the following expressions are obtained.

$$c = \sqrt{\left[\frac{g(\rho_2 - \rho_1)h_1 h_2}{\rho_2 h_1 + \rho_1 h_2} \right]} \tag{9}$$

$$\alpha = \frac{3c(\rho_2 h_1^2 - \rho_1 h_2^2)}{2h_1 h_2(\rho_2 h_1 + \rho_1 h_2)} \tag{10}$$

$$\gamma = \frac{c h_1 h_2(\rho_1 h_1 + \rho_2 h_2)}{6(\rho_2 h_1 + \rho_1 h_2)} \tag{11}$$

where h_1 and ρ_1 are the thickness and density of the upper layer while h_2 and ρ_2 are the thickness and density of the lower layer. The final model for the first mode is presented below

$$\eta(x,z,t) = \eta_0 W(z) I(x,t) \left\{ 2dn_s^2 \left[\frac{1}{2} k_0(x - Vt) \right] - 1 + s^2 \right\} \tag{12}$$

The first mode is considered in this paper as it is the most prevalent and has the highest velocities associated among all the modes. The velocities and accelerations can be obtained by utilizing the continuity equation and the nonlinear kinematic boundary condition (Apel 2003).

4. Internal Solitons in the South China Sea

Internal waves are commonly seen in the South China sea and have been extensively studied (Liu *et al*. 2008 and Liu and Hsu 2009) The Luzon Strait is found to be the main source of generation of internal waves in the S China Sea (Ko *et al*. 2008). The energy sources for these waves, with amplitudes up to 200 m, are the semidiurnal tides and the Kuroshio current with the former most prevalent. It is seen that the ocean tides are converted by the ridge into internal tides which due to nonlinear effects are transformed into undular bores. These lead to the formation of an internal wave train that propagates west towards Dongsha Island (Fig. 1).

5. Environmental parameters

The environment considered in this study is based on a realistic floating platform design operation/survival conditions and internal waves observed in South China Sea.

4.1 Field description

The South China Sea Liwan 3-1 field, a large gas reservoir with potential reserves of 6Tcf was discovered in 2006. The field is situated on Block 29/26 approximately 350 km SE of Hong Kong and spans 979,773 acres (3,965 square kilometers). In this study, it is assumed that the site water depth is 1219 m (4000ft) and the pycnocline is at 200 m below the surface.

4.2 Surface wave, wind and current

The summary of regular environmental conditions applied in the analysis is presented in Table 1. These correspond to waves with return period of 100-year and 1-year respectively.
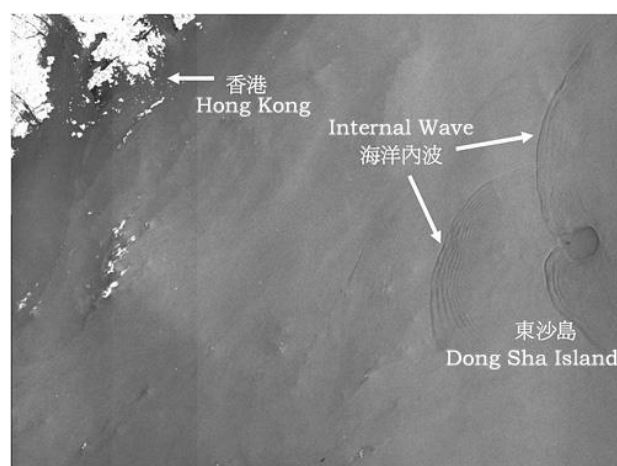
Fig. 1 Internal waves near Dong Sha Island in the S China Sea. (© Hong Kong Chinese University
        Satellite Observation, Nov, 2006)

Table 1 Summary of Environmental Conditions

Items		South china Sea Water Depth = 1219.2 m					
		1		2		3	
		100-year Hurricane				1-year Return Period Criteria	
		Wave Dominant		Wind Dominant			
		Design Extreme		Design Extreme		Maximum Operating	
Wave		Jonswap		Jonswap		Jonswap	
Gamma		2.4		2.4		1	
Wave Direction	(deg)	180		180		108	
Significant (Hs)	(ft)	15.24		14		6	
Spectral Peak Priod (Tp)	(s)	15.6		15.1		11.2	
Wind		API		API		API	
1 hour Avg. Wind	(ms)	42.98		45		21.97	
Wind Direction	(deg)	180		180		180	
Current Profile		Normal		Normal		Normal	
		Depth	Vel	Depth	Vel	Depth	Vel
		(m)	(m/s)	(m)	(m/s)	(m)	(m/s)
		0	1.91	0	2	0	1.02
		-36.88	14	-36.88	1.47	-50	0.77
		-75	0.19	-75	0.19	-100	027
		-1219.2	0.19	-1219.2	0.19	-1219.2	0.13
Current Direction	(deg)	180		180		180	

Table 2 Internal Wave Input Parameters

Parameters	Unit	Case 1	Case 2
Internal Wave Height	m	90	170
Upper Layer Depth	m	200	200
Upper Layer Fluid Density	kg/m^3	1020	1020
Lower Layer Depth	m	1019.2	1019.2
Lower Layer Fluid Density	kg/m^3	1028	1028
Internal Wave Pre-existing Time T_0	sec	30000	10000
Recovery Function Power (A)	-	4	4
Error Function β	-	3.0	3.0
Error Function φ	-	-0.1	-0.1
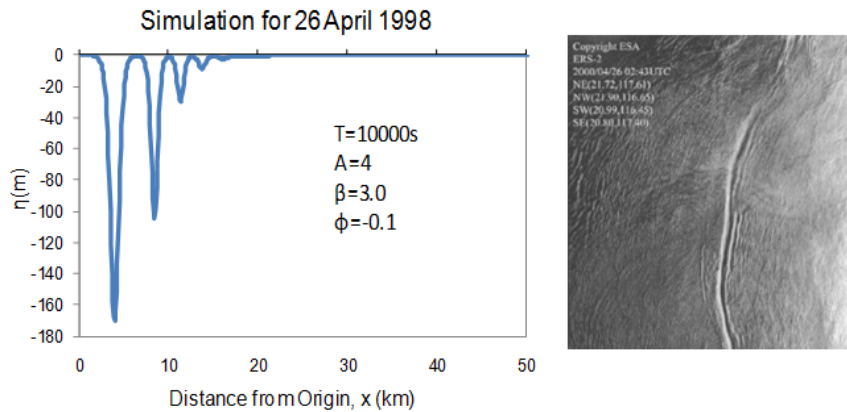
Fig. 2 Internal Wave Model and the Corresponding Satellite Picture (April 26, 1998)

4.3 Internal wave

The internal wave model shown in Fig. 2 (left) is created based on a satellite picture (Fig. 2, right) taken on April 26, 1998. It has a representative shape and basic characteristics of internal waves observed in South China Sea near the Liwan gas field. Two sets of internal waves, summarized in Table 2, are generated for the analysis. The 90 m wave is considered to an intermediate internal wave in the South China Sea while the 170 m wave corresponds to an extreme wave.

It is assumed that the internal wave may occur up to the maximum operating wave condition for the platform design and analysis. Internal wave is not applied during the survival environmental condition, and it is analyzed for comparison purpose only.

The duration between the 1st peak and 2nd peak is 26.5 minutes for the 170 m wave while it is 16.7 minutes for the 90 m wave. The duration between the 2nd peak and 3rd peak is 18.3 minutes and 11.8 minutes for the 170 m and the 90 m internal waves respectively. The internal wave developing time (T_0) before the start of the coupled analysis is 30,000 seconds and 10,000 seconds for the 90 m and the 170 m internal wave. This time is selected to form a desired geometry of the internal wave based on observable data for coupled analysis. The internal group speed and the maximum velocity obtained at the sea water surface are summarized in Table 3. Although the amplitude of the internal wave sounds scary, its induced particle velocities are not that large, as can be seen in Table 3. The feature and order of magnitude of the induced horizontal velocities are similar to those of loop current in the GoM.

The time history of the internal wave height and scaled velocities distributions are presented in Figs. 3 to 5. It is seen that the horizontal velocity is positive above the pycnocline while it is negative below the pycnocline. The horizontal velocity is directly proportional to the vertical rate of change of the structure function which causes this shearing effect near the pycnocline. The internal wave velocities have much higher magnitude compared to the accelerations and thus have a much more contribution to the platform motions.

Nishu V. Kurup, Shan Shi, Lei Jiang and M.H. Kim

Internal Wave Height
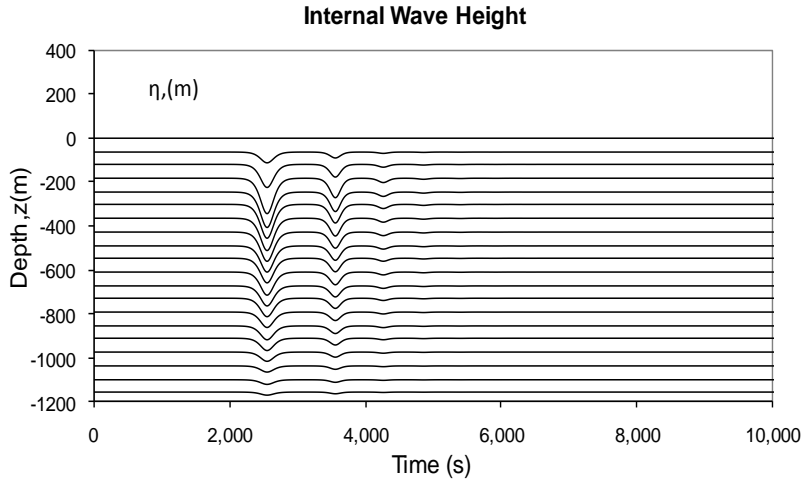
Fig. 3 Internal Wave Height Distribution with Depth (η=170 m)

Horizontal Velocity
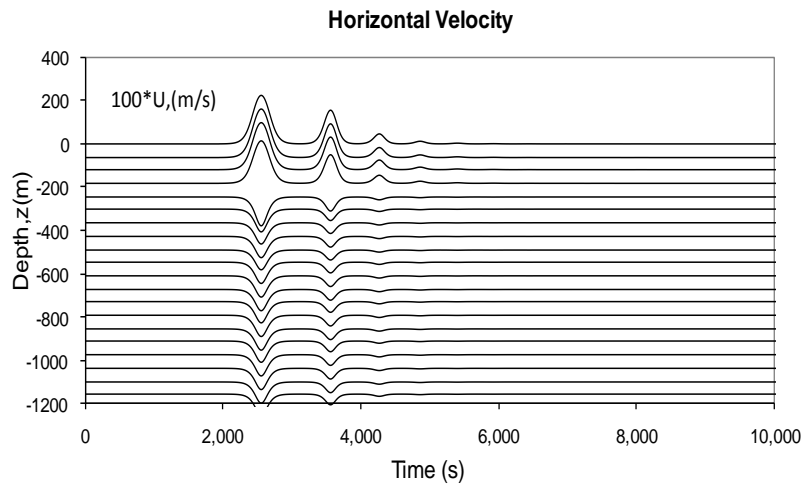
Fig. 4 Horizontal Velocity Distribution with Depth (η=170 m)

Table 3 Group Speed and Maximum Horizontal Velocity

Wave Height (m)	Group Speed (m/s)	Max. Hori. Velocity (m/s)
90	3.58	1.31
170	3.58	2.21
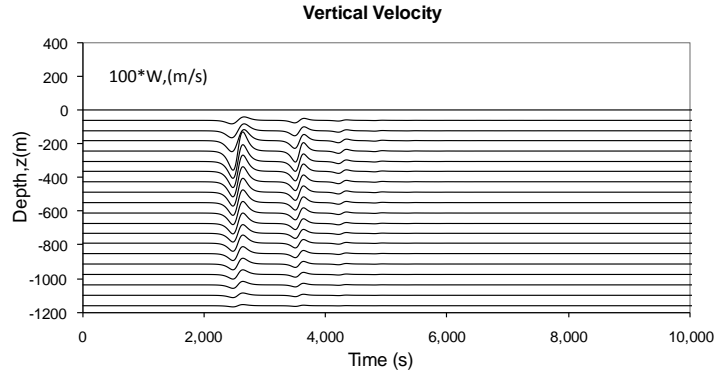
Fig. 5 Vertical Velocity Distribution with Depth (η=170 m)

5. Coupled analysis and modeling

Coupled hull hydrodynamics, mooring and riser program HARP is modified to perform time domain global analysis with the developed internal wave. The program applies the wave radiation/diffraction forces calculated by program WAMIT, and perform nonlinear dynamic finite element analysis to evaluate the strength of flexible risers and moorings coupled with floating platform motions. The internal wave kinematics has been included in the Morison drag model. Calculation flow chart of the program is shown in Fig. 6 below
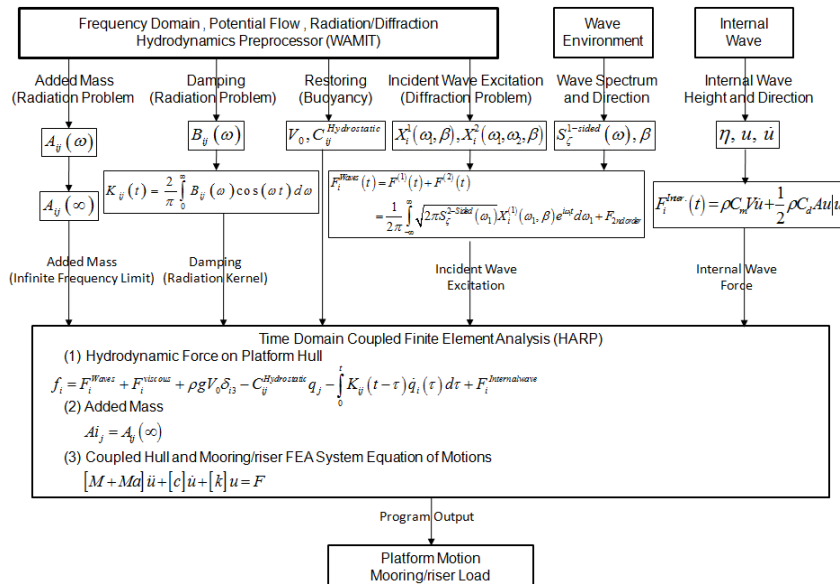
Fig. 6 Summary of Program HARP Calculations
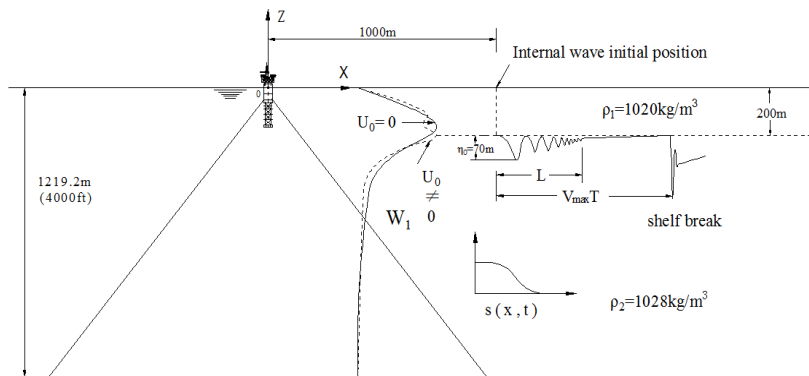
Fig. 7 Coupled Analysis Models in HARP and Internal Wave Initial Setup

A Spar platform designed for the same field with compatible process capability is used in the study. The coupled analysis model includes the platform hull, mooring lines and risers. The moorings and risers are connected to the Spar hull using springs with corresponding stiffness. The portions of the mooring chain and SCR(steel catenary riser) on the seabed are modeled with contact springs to simulate the soil stiffness and drag. Fig. 7 demonstrates the internal wave initial setup relative to the platforms coupled analysis model. The front of the internal wave at the beginning of simulation is 1000 m away from the platform origin. The structure function $W(z)$ which represents the distribution of the internal wave along the water depth is also shown in the same figure.

6. Spar production system

6.1 Spar description

The production truss spar key figures are summarized in Table 4 below

The spar configuration and the mooring line properties are shown in Fig. 8 and Table 5 respectively.

The Spar coupled analysis model and the hydrodynamic panel model used by the wave diffraction and radiation program WAMIT are presented in Figs. 9 and 10. The hull and heave plates are modeled with 3040 panels. The truss members and hull had a drag coefficient of 1.2 while a drag coefficient of 10 was used for the heave plates. Newman's approximation where the QTFs are based on the mean drift forces has been applied in the analysis. Twelve taut chain-polyester-chain mooring lines in four sets of three each have been modeled for station keeping purpose. The mooring lines were modeled with 15 higher order elements with a drag coefficient of 1.2 for the wire section and 2.4 for the chain section. The analysis model also includes 8 production TTRs (Top-Tensioned Risers), 1 drilling riser, 2 import SCRs (Steel Catenary Risers), and 2 export SCRs.

Table 4 Spar Key Figures

Draft	m	164.59
Displacement (including entrapped water)	N	8.69×10^8
Total Weight (including entrapped water)	N	7.73×10^8
Hard Tank Diameter	m	37.19
Hard Tank Height above MWL	m	16.76
Hard Tank Height below MWL	m	63.09
Center Well Dimension	m	10.97×10.97
Main Truss Member Length	m	97.49
Heave Plate Dimension	m	37.19×37.19
Heave Plate Height	m	1.0
Number of Heave Plates	-	3
Soft Tank Dimension	m	37.19×37.19
Soft Tank Height	m	6.1
Vertical C.G. from Base KG	m	98.66
Vertical C.B. from Base KB	m	109.0
Pitch Radii of Gyration Rxx	m	77.12
Roll Radii of Gyration Ryy	m	77.27
Yaw Radii of Gyration Rzz	m	14.63

Table 5 Spar Mooring Line Properties

Mooring Line Properties	Diameter (m)	EA (KN)	Breaking Strength (KN)	Wet Weight (Kg/m)	Dry Weight (Kg/m)	Length (m)
Chain	0.1334	2.06	15746	309.39	355.62	121.9
Polyester	0.22	4.10	14168	8.53	32.72	1388.4
Chain	0.1334	2.06	15746	309.39	355.62	304.8

6.2 Spar analysis and results

Three-hour time domain dynamic analyses are performed for both internal wave heights of 90m and 170 m. The operational and survival conditions are also analyzed without the presence of internal waves for comparison. The Spar motions and the top tension time histories of the mooring line (#5) subject to the highest loads for the 170 m height internal wave are shown in Figs.11 to 14. The motion statistics and the maximum mooring line tension with corresponding utilization ratios are summarized in Tables 6 and 7 respectively.
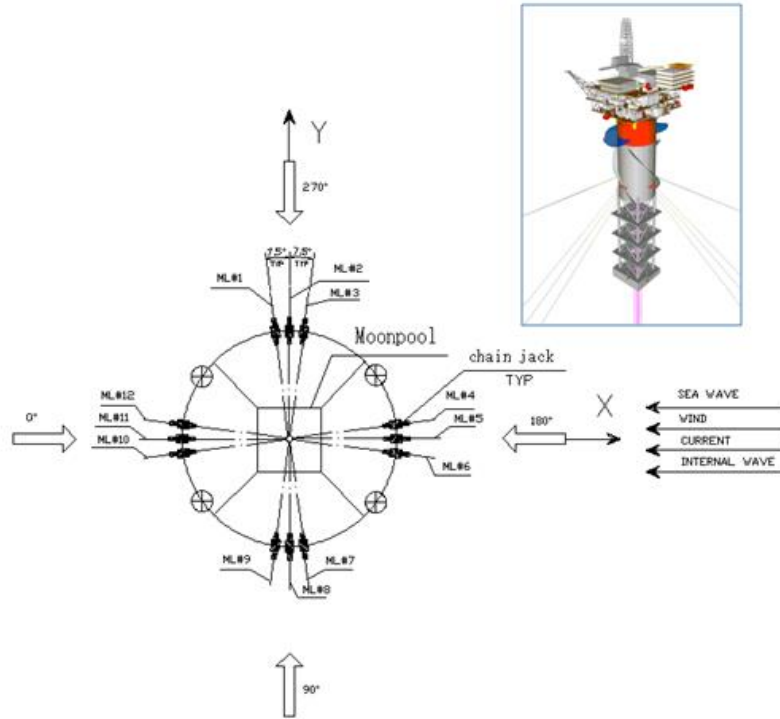
Fig. 8 Spar Configuration and Mooring Layout
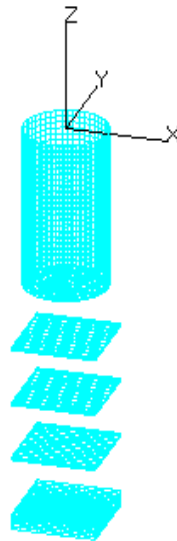
Fig. 9 Panel Model of Spar
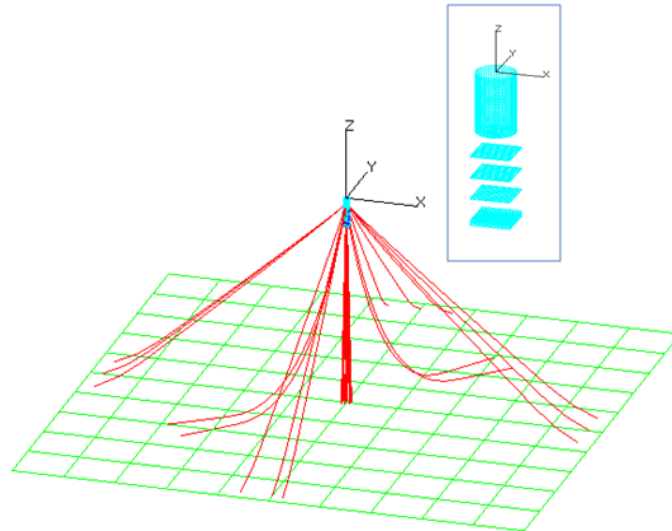
Fig. 10 Spar Coupled Analysis Model with Program HARP

In general, the front peak is the most important. The next peak is smaller but also significant. The maximum pitch with internal wave is smaller than that of survival condition but it can heel about 4 degrees for many minutes, which can cause some concern for topside-facility operations. The surge offset is significantly increased with the internal wave compared to the survival condition, which may be a concern for riser and mooring safety, as can be seen in Table 7.
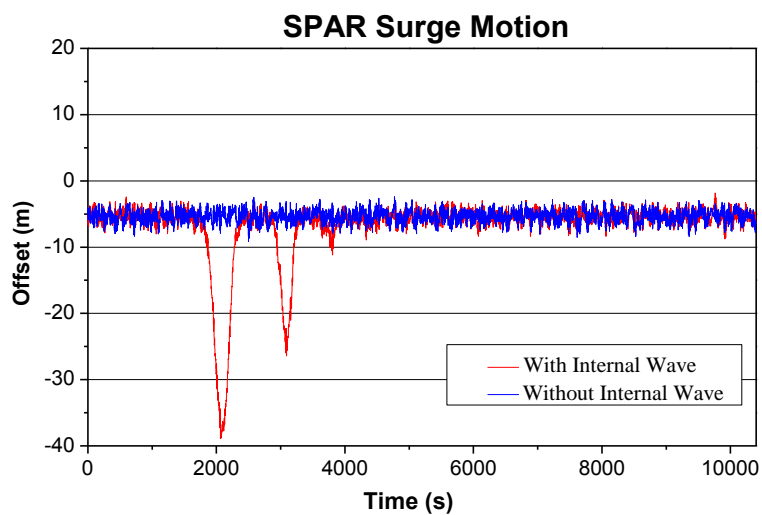
Fig. 11 Spar Surge Motion Time History (η=170 m)
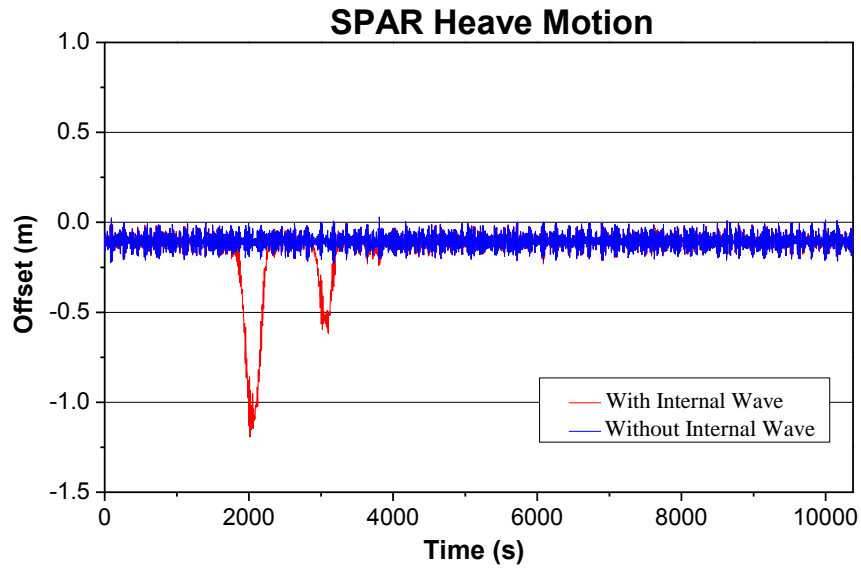
Fig. 12 Spar Heave Motion Time History (η=170 m)
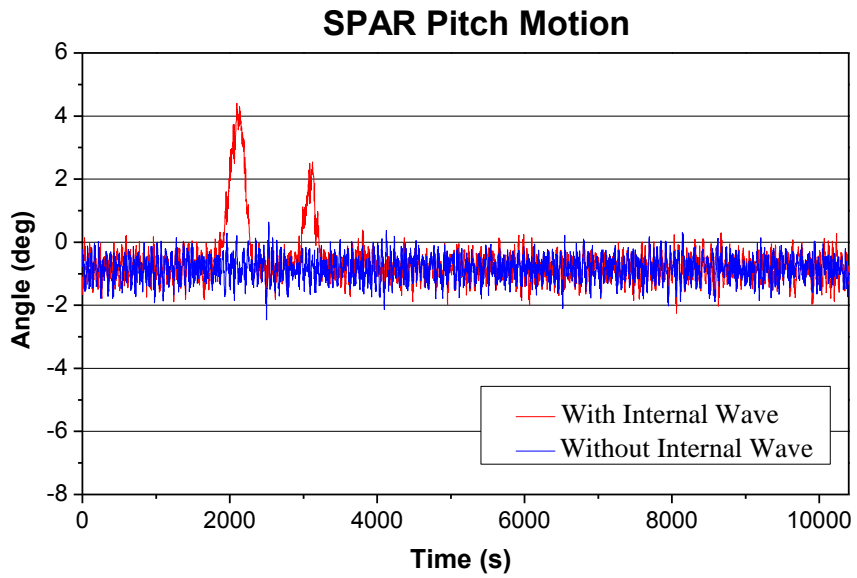
Fig. 13 Spar Pitch Motion Time History (η=170 m)

Table 6 Spar Motion Statistics

Condition			Operation			Survival	
						Wave Dominant	Wind Dominant
Internal Wave Height			N/A	90m	170m	N/A	N/A
Offset	MAX	m	-2.42	-2.48	-1.77	-5.59	-7.11
	MIN	m	-9.13	-21.29	-39.05	-29.32	-29.69
	MEAN	m	-5.38	-6.17	-6.56	-15.33	-16.36
Heave	MAX	m	0.03	0.03	0.01	1.88	1.46
	MIN	m	-0.23	-0.51	-1.18	-2.23	-1.90
	MEAN	m	-0.11	-0.12	-0.14	-0.21	-0.23
Pitch	MAX	deg	0.63	2.24	4.38	1.04	0.91
	MIN	deg	-2.46	-2.46	-2.20	-6.86	-6.92
	MEAN	deg	0.36	-0.73	-0.65	-2.48	-2.68

Table 7 Spar Mooring Line #5 Max Tension and Utilization Ratio

Condition		Operation			Survival	
					Wave Dominant	Wind Dominant
Internal Wave Height		N/A	90 m	170 m	N/A	N/A
Line Max Tension	KN	4.00E+03	6.37E+03	1.01E+04	7.51E+03	7.52E+03
Utilization Ratio (Max Tension/Min Breaking Tension)	-	0.28	0.45	0.71	0.53	0.53
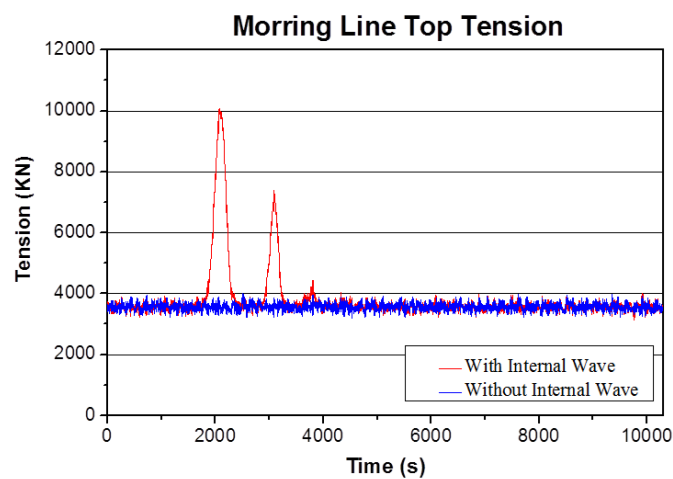
Fig. 14 Spar Mooring Line #5 Top Tension Time History (η=170 m)

7. Conclusions

The internal wave model presented in this study and the analysis method could provide relatively realistic representation of internal waves observed in South China Sea for offshore engineering project applications. It is also observed that the internal wave impact on platform motions and mooring/riser strength can be analyzed separately and superimposed to the wind and wave analysis results due to the long period nature of internal waves.

It is seen that internal waves have significant impact on Spar offset, heave, and pitch motions. The Spar offset for the 170 m internal wave is larger than its design offset from survival condition, which also results in larger mooring loads and utilization ratios. Our results indicate that the Spar will pitch 2.24 degree and 4.38 degree in the internal wave incident direction for several minutes for the 90 m and the 170 m internal waves respectively. It is thus recommended that Top-tensioned risers on Spar platforms should be designed with the consideration of the large offset of the platform due to the presence of internal wave.

Acknowledgments

References

Apel, JR (2003), "A new analytical model for internal Solitons in oceans", *J. Phys. Oceanography*, **33**, 2247-2269.

Armi, L, and Farmer, DM (1988), "The flow of Mediterranean water through the Strait of Gibralter", *Prog. Oceanogr.*, **21**, 1-105.

Benjamin, T.B. (1966), "Internal waves of finite amplitude and permanent form", *J. Fluid Mech.*, **25**(2), 241-270.

Choi, W. and Camassa, R. (1999), "Fully nonlinear internal waves in a two-fluid system", *J. Fluid Mech.*, **396**, 1-36.

Duda, T, and Farmer, D, (Eds) (1999), *The WHOI/IOS/ONR Internal Solitary Wave Workshop: Contributed Papers*, Technical Report WHOI-99-07.

Goff, M., Jeans, G., Harrington-Missin, L. and Baschenis, C. (2010), "Soliton early warning system for offshore applications", *Proceedings of the Ocean Observation and Forecasting*, Oceanology International Conference.

Gurevich, A.V. and Pitaevskii, L.P. (1973a), "Nonstationary structure of a collisionless shockwave", *Sov. Phys. JETP*, **38**, 291-297.

Gurevich, A.V. and Pitaevskii, L.P. (1973b), "Decay of initial discontinuity in the Korteweg- De Vries equation", *JETP Lett. V.*, **17**, 193-195

Huang, W., You, Y. and Li, W. (2015), "Predicting internal solitary wave loads on spar platforms", *Proceedings of the Offshore Technology Conference*, OTC-25904-MS, Houston Texas, USA.

Joseph, R.I. (1977), "Solitary waves in a finite depth fluid", *J. Phys. A: Math Gen.*, **10**(12), 225-227.

Ko, D.S., Martin, P.J., Chao, S.Y., Shaw, P.T. and Lien, R.C. (2008), "Large Amplitude Internal Waves in the South China Sea", *Ocean Sci. Technol.*, NRL Review, 197-200.

Koop, C.C. and Butler, G. (1981), "An investigation of internal solitary waves in a two fluid system", *J. Fluid Mech.*, **112**, 225-251.

Korteweg, DJ, and de Vries, G (1895), "On the change of form of long waves advancing in a rectangular canal, and on a new type of long stationary wave", *Philos. Mag.*, **39**, 422-443.

Kubota, T., Ko, D.R.S. and Dobbs, L. (1978), "Propogation of weakly nonlinear internal waves in a stratified fluid of finite depth", *J. Hydrodynamics*, **12**, 157-165.

Kurup, N.V., Shi, S., Shi, Z., Miao, W. and Jiang, L. (2011), "Study of nonlinear internal waves and impact on offshore drilling units", *Proceedings of the ASME 2011 30th International Conference on Ocean*, Offshore and Arctic Engineering, Rotterdam, The Netherlands, June.

Liu, A.K., Holbrook, J.R. and Apel, J.R. (1985), "Nonlinear internal wave evolution in Sulu sea", *J. Phys. Oceanography*, **15**, 1613-1624.

Liu, A.K., Hsu, M.K. and Zhao, Y. (2008), "Overview of Internal Waves in the South China Sea", Chapter I, *Satellite Remote Sensing of South China Sea*, (Eds., A.K. Liu, C.R. Ho and C.T. Liu), Tingmao Publish Co., Taipei.

Liu, A.K. and Hsu, M.K. (2009), "Satellite remote sensing of nonlinear internal waves in the South China Sea", *Proceedings of the ISOPE International Deep-Ocean Technology (IDOT) Symposium*, Beijing, China.

Miyati, M. (1985), "An internal solitary wave of large amplitude", *La Mer*, **23**, 43-48.

Ono, H. (1975), "Algebraic solitary waves in stratified fluids", *J. Phys. Soc. Japan*, **39**, 1082-1091.

Osbourne, A.R., Brown, J.R., Burch, T.L. and Scarlet, R.I. (1977), "The influence of internal waves on deepwater drilling operations", *Offshore Technol. Conference*, **2797**, 537-541.

Ostrovsky, L.A. and Stepanyants, Y.A. (1989), "Do internal Solitons exist in the ocean?", *Rev. Geophys.*, **27**(3), 293-310.

Segur, H. and Hammack, J.L. (1982), "Soliton models of long internal waves", *J. Fluid. Mech.*, **118**, 285-304.

Shi, S., Kurup, N.V., Halkyard, J. and Jiang, L. (2013), "A study of internal wave influence on OTEC systems", *Ocean Syst. Eng.*, **3**(4), 309-325.

Sun, M. and Huang, W. (2012), "A new concept of spar in deep water and its hydrodynamic performance under internal wave", *Proceedings of the 22nd International Offshore and Polar Engineering Conference*, Rhodes, Greece, June.

Xu, W., Li, Y. and Voogt, A. (2013), "Internal wave soliton passage simulation during offloading", *Proceedings of the ASME 2013 32nd International Conference on Ocean*, Offshore and Arctic Engineering, Nantes, France, June.

Zhang, H.Q. and Li, J.C. (2007), "Wave loading on floating platforms by internal solitary waves", *Proceedings of the 5th International Conference on Fluid Mechanics*, Shanghai, China, Aug.